Molecular Catalysis 438 (2017) 130–142

Contents lists available at ScienceDirect

Molecular Catalysis

journal homepage: www.elsevier.com/locate/mcat

MCAT

Insight into the properties of stoichiometric, reduced and sulfurized CuO surfaces: Structure sensitivity for H_2S adsorption and dissociation

Jin Zhang[a], Miaoqing Liu[a], Riguang Zhang[a,*], Baojun Wang[a], Zaixing Huang[b]

[a] Key Laboratory of Coal Science and Technology of Ministry of Education and Shanxi Province, Taiyuan University of Technology, Taiyuan 030024, Shanxi, PR China

[b] Department of Chemical and Petroleum Engineering, The University of Wyoming, Laramie, WY 82071, USA

ARTICLE INFO

Article history:
Received 22 March 2017
Received in revised form 8 May 2017
Accepted 22 May 2017

Keywords:
H_2S
Adsorption
Dissociation
CuO(111)
Density functional theory

ABSTRACT

A mechanistic and kinetic study about the adsorption and dissociation of H_2S on different types of CuO(111) surfaces, including the stoichiometric, reduced and sulfurized surfaces, has been carried out to probe into the structure sensitivity for H_2S adsorption and dissociation. Here, density functional theory calculations have been employed. Our results show that sulfur-containing species (H_2S, SH and S) dominantly interact with the surface Cu via S atom, and H is mainly adsorbed at the outermost surface oxygen site. H_2S dominantly exists in the form of dissociative adsorption leading to SH and H species, meanwhile, a small quantity of molecular adsorption H_2S also exist on these surfaces. The complete dissociation of molecular adsorption H_2S on three CuO(111) surfaces clearly show that the overall dissociation process is exothermic, the stoichiometric surface is the most favorable; the sulfurized surface suppresses the H—S bond activation and dissociation. Consequently, the catalytic activity toward molecular adsorption H_2S dissociation follows the order: Stoichiometric > Reduced > Sulfurized surface, which have been also confirmed by projected density of states (pDOS), *d*-band analysis, and the inter-atomic distances. Therefore, H_2S dissociation over CuO(111) surface is a structure-sensitive reaction, the effect of surface structure on H_2S adsorption and dissociation may play an important role in improving high-performance H_2S gas sensors, in which molecular adsorption H_2S can be detected on the sulfurized surfaces. In addition, the vibrational frequencies of the adsorbed H_2S and SH species on these surfaces can provide a theoretical guidance for the experimental vibrational spectroscopy.

1. Introduction

Acquiring a fundamental understanding about H_2S interaction with the solid surfaces is crucial based on several reasons, firstly, most catalysts are deactivated or poisoned rapidly by H_2S and SO_2 in the process of heterogeneous catalysis [1–6]; secondly, H_2S is the most common impurities or byproduct in syngas, fossil fuels, chemical feedstock and natural gas; thirdly, metal oxides are widely selected as the sorbents to remove H_2S [7–9]. Thus, the studies about H_2S interaction with the metal oxides can provide fundamental insights into the poisoning effect of catalysts, and provide a clue for designing H_2S gas sensing [10–12].

Nowadays, theoretical and experimental studies about H_2S interaction with metal oxides, including CuO [11–15], Cu_2O [16–18], MgO [19], Al_2O_3 [20], ZnO [21], CeO_2 [22], ZrO_2 [23], etc., have been investigated, indicating that H_2S, SH and S species mainly interact with surface metal. For different metal oxides, copper-based oxides (Cu_2O and CuO) have been widely used due to the low cost and relatively high activity toward H_2S dissociation.

For Cu_2O surface, previous experimental studies [16] indicated that H_2S dissociative adsorption mainly attributes to the chemical properties of exposed surface rather than the reaction conditions. Then, the experimental studies by Lin et al. [17] showed that H_2S dissociation into SH species is spontaneous on $Cu_2O(111)$ surface. Meanwhile, density functional theory (DFT) studies [18] investigated the adsorption of H_2S on $Cu_2O(111)$ surfaces with different surface structures, suggesting that H_2S is the dissociative adsorption on the reduced surface, and the existence of surface S atom goes against the break of H—S bond on the sulfurized surface.

For CuO surfaces, Ramgir and Steinhauer et al. [11,12] have proposed that CuO presents a better response to H_2S gas sensing, which is used as an ideal material with high selectivity for H_2S gas sensing. Then, the experimental studies [16] confirmed that H_2S is the dissociative adsorption on CuO surface, which depends on the chemical nature of exposed surface. Meanwhile, CuO-based sorbents are highly efficient to remove H_2S [13,14]. However, the underlying mechanism of H_2S interaction with CuO surface is still unclear at a

* Corresponding author.
E-mail addresses: zhangriguang@tyut.edu.cn, zhangriguang1981@163.com (R. Zhang).

http://dx.doi.org/10.1016/j.mcat.2017.05.020
2468-8231/

molecular level; up to now, to the best of our knowledge, only Sun et al. [15] have reported the adsorption and dissociation of molecular adsorption H_2S on the stoichiometric CuO(111) surface using DFT calculations, suggesting that S and H species are the most favorable products, however, H_2S dissociative adsorption has not been identified.

In reality, the oxygen-vacancies on metal oxide surfaces are easily formed, which leads to the surface reduction, and further alter the catalytic reactivity [24]. Recent studies [25] have shown that the reduction of CuO(111) surface leads to the lower activation barrier of H_2O dehydrogenation compared to the stoichiometric surface. DFT studies [21] found that the surface reduction on ZnO(10-10) surface contributes to H_2S dissociative adsorption, and the dissociated S atom prefers to adsorb at the reduced surface rather than the stoichiometric surface. On the other hand, the effect of surface modification by S atoms on H_2S adsorption and dissociation has been investigated on Au surfaces, indicating that the presence of S atom promotes the first H—S bond-breaking of H_2S, and resists the dissociation of SH group [26]. Yet, few studies about the H—S bond activation of H_2S on the sulfurized CuO(111) surface have been reported until now. Therefore, the behaviors of H_2S adsorption and dissociation on the reduced and sulfurized CuO surfaces are still ambiguous, it is necessary to probe into H_2S adsorption and dissociation on different CuO(111) surfaces, as well as the effect of surface structure on H_2S adsorption and dissociation.

Due to the rapid dissociation of H_2S in the experimental process, some important issues, such as the adsorption configurations and dissociation pathways of H_2S on metal oxide surfaces, fail to be fully characterized; nowadays, DFT calculations have been proved to be a powerful technique to explore the adsorption and dissociation of small molecules on the solid surfaces, which can well illustrate the underlying mechanism [15,18,21]. Thus, DFT calculations about the behavior of H_2S adsorption and dissociation on the surfaces of metal oxide are valuable.

CuO(111) surface is the most stable and the dominantly exposed surface of CuO under the realistic conditions, which has been widely employed as an ideal model to investigate the chemical properties [15,25,27,28]. Importantly, recent experimental studies showed that CuO(111) surface exhibits the predominant surface catalytic activity toward H_2S dissociation [29]. Therefore, in this study, three types of CuO(111) surfaces, including the stoichiometric, reduced and sulfurized surfaces, have been employed to probe into the effect of surface structure on the behavior of H_2S adsorption and dissociation using DFT calculations. The adsorption energies and the stable adsorption configurations of H_2S, SH, S and H species have been firstly examined over different CuO(111) surfaces; then, a mechanistic and kinetic study about the complete dissociations of molecular adsorption H_2S have been investigated, and the energetic of every elementary step is analyzed. Further, the effect of CuO(111) surface structures on the behaviors of H_2S adsorption and dissociation have been discussed on the basis of the electronic properties, H—S bond length, and charge transfer. Finally, the surface structure sensitivity can be identified.

2. Computational details

2.1. Surface models

The six-layered CuO(111) surface model is built, and a $p(3 \times 2)$ super-cell is employed corresponding to a coverage of 1/6 ML, which can well avoid the lateral interaction of adsorbed species, the details about the evaluation of surface models are shown in Part 1 of the Supplementary Material. The bottom three layers of the substrate are kept fixed to maintain the bulk crystal structure, while the top three layers of the substrate and adsorbed species are allowed to relax. Meanwhile, a vacuum space of 10 Å is added perpendicular to the surface in order to avoid the interactions between the periodic configurations. This model has been widely used in the previous theoretical studies about small molecular interactions with metal surfaces [15,25,27,30]. Meanwhile, the removal of one surface O atom and the pre-covered of one S atom on the stoichiometric surface is employed to model the reduced and sulfurized surfaces, respectively, the detailed information about the surface models and the corresponding adsorption sites are presented in Part 2 of the Supplementary Material.

2.2. Calculation methods

DFT together with a van der Waals-inclusive dispersion correction (DFT-D) have been employed to perform all calculations to improve the description of the weak interaction [15,31]. The main calculations presented here are based on the generalized gradient approximation (GGA) of Perdew and Wang (PW91) exchange-correlation functional [32–34]. The dispersion correction scheme proposed by Ortmann, Bechstedt, and Schmidt (OBS) is employed within DFT-D [31]. The inner electrons of Cu atoms are kept frozen and replaced by a DFT Semi-core Pseudopots (DSPP), and other atoms are treated with an all-electron basis set. The double-numerical basis with polarization functions (DNP) is applied to expand the valence electrons functions [35,36]. A Monkhorst-Pack grid of $3 \times 3 \times 1$ and a Methfessel-Paxton smearing of 0.005 Ha [25] have been performed. As shown in Part 3 of the Supplementary Material, our test results indicate that the chosen method and model are suitable for describing the behaviors of H_2S adsorption and dissociation on CuO(111) surface. All calculations are implemented in $Dmol^3$ program package of Materials Studio 8.0 [37,38].

All energies with the zero-point vibrational corrections are obtained at T = 475 K, since it has been proved that CuO exhibits the optimum activation energy toward H_2S at this temperature [29]. The computational details about free energy change ($\Delta_r G_m$) and activation free energy ($\Delta_r G_m^{\neq}$) of the elementary reaction, as well as the adsorption free energy (G_{ads}) are shown in Part 4 of the Supplementary Material.

3. Results and discussion

3.1. The adsorption of atomic H, S and SH species

The adsorption of H, S and SH species on CuO(111) surface have been examined. On the stoichiometric CuO(111) surface, eight different adsorption sites have been considered, as shown in Fig. S1(a); On the reduced and sulfurized surfaces, as presented in Fig. S1(b) and (c), $O_{vacancy}$ and S_p sites have also been considered, respectively.

3.1.1. Atomic H adsorption

For the adsorption of atomic H on the stoichiometric surface, it is found that the models of H initially adsorbed at O_{SUF}–O_{SUF} and Cu_{SUF}–Cu_{SUF} bridge sites are all optimized to that adsorbed at O_{SUF} site, as shown in Fig. 1(a). Meanwhile, H initially adsorbed at $O_{vacancy}$ site is converted to Cu^2–Cu^3 bridge site, as presented in Fig. 1(b). Further, H atom can also stably adsorb at the S_p site on the sulfurized surface, as shown in Fig. 1(c).

The free energy of H adsorption at different sites could be assigned in the following order: S_p (327.6 kJ mol^{-1}) > O_{SUF} (300.1 kJ mol^{-1}) > O_{SUB} (296.5 kJ mol^{-1}) > Cu^2–Cu^3 (261.5 kJ mol^{-1}) > Cu_{SUB}–Cu_{SUB} (178.1 kJ mol^{-1}) > Cu_{SUB} (157.3 kJ mol^{-1}) > Cu_{SUF} (100.0 kJ mol^{-1}), suggesting that O_{SUF} is the most favorable site for H adsorption on the stoichiometric and reduced surfaces [25], while S_p is the dominate active center for H adsorption on the sulfurized surface.

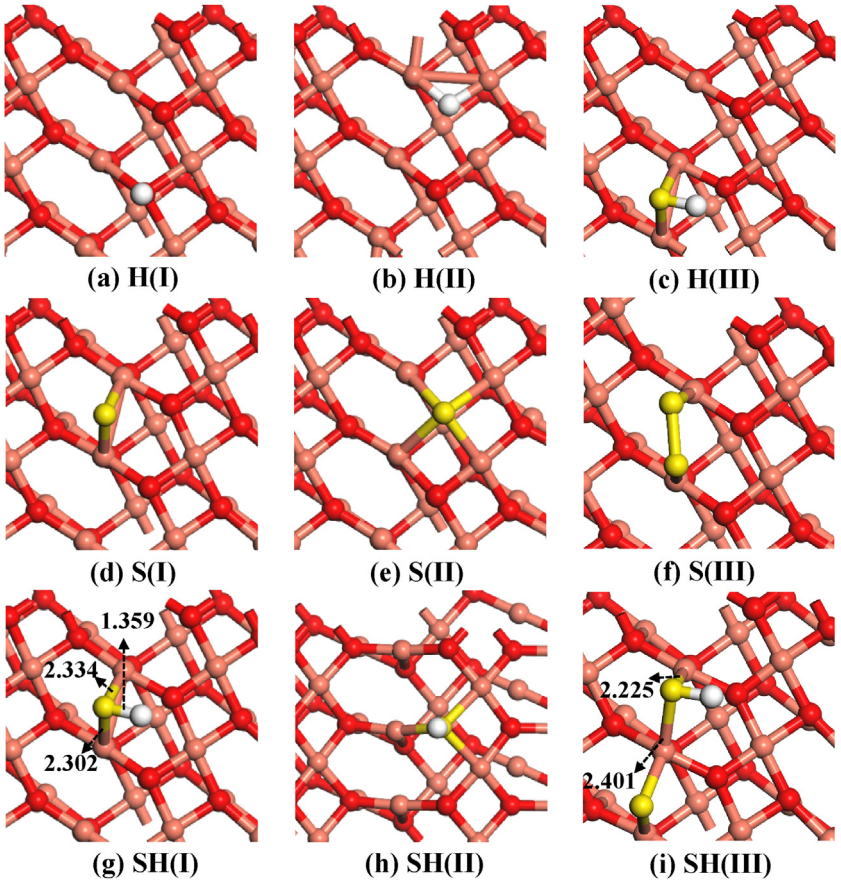

Fig. 1. Optimized adsorption configurations of H, S and SH species on CuO(111) surface. (I), (II) and (III) represent the stoichiometric, reduced and sulfurized surface, respectively. Orange, red, yellow, white and black balls stand for Cu, O, S, H atoms and the oxygen-vacancy site, respectively. Bond lengths are in Å. (For interpretation of the references to colour in this figure legend, the reader is referred to the web version of this article.)

3.1.2. Atomic S adsorption

For the adsorption of atomic S on the stoichiometric and reduced surfaces, a single S atom initially placed at nine different adsorption sites has been examined. Besides $O_{vacancy}$ site, S initially adsorbed at other eight sites are all converted to the Cu_{SUB}–Cu_{SUB} bridge site; Thus, only two stable adsorption configurations have been obtained, as shown in Fig. 1(d) and (e). Atomic S on the stoichiometric surface is adsorbed at the Cu_{SUB}–Cu_{SUB} bridge site with an adsorption free energy of 242.0 kJ mol^{-1}, while S atom fills the $O_{vacancy}$ site on the reduced surface with the adsorption free energy of 374.3 kJ mol^{-1}. Above results indicate that Cu_{SUB}–Cu_{SUB} bridge site and $O_{vacancy}$ site are the active centers for atomic S adsorption on the stoichiometric and reduced surfaces, respectively.

On the sulfurized surface, only Cu_{SUB}–Cu_{SUB} bridge site is examined, since it is also only the active center on the stoichiometric surface. The optimized configuration, as shown in Fig. 1(f), the S—S bond is formed, and two S atoms are all adsorbed at Cu_{SUB} site, which means that S is easily aggregated on the sulfurized surface.

3.1.3. SH adsorption

For the adsorption of SH on the stoichiometric and reduced surfaces, we examined two molecular orientations of H-down and S-down over nine adsorption sites. Interestingly, the optimized results show that all H-down models are completely converted to S-down modes.

For S-down adsorption, two stable adsorption configurations (see Fig. 1(g) and (h)) are obtained, in which SH is adsorbed at the Cu_{SUB}–Cu_{SUB} bridge site on the stoichiometric surface with the H—S bond length of 1.359 Å, and that at $O_{vacancy}$ site on the reduced surface with the H—S bond length of 1.358 Å; both have the adsorption free energies of 208.5 and 305.3 kJ mol^{-1}, respectively.

Above results show that SH adsorbed at the Cu_{SUB}–Cu_{SUB} bridge site via S-down mode is the most stable on the stoichiometric surface, thus, in the case of SH adsorption on the sulfurized surface, Cu_{SUB}–Cu_{SUB} bridge and Cu_{SUB} sites via S-down mode are examined, and only one stable adsorption configuration is obtained, as shown in Fig. 1(i), which is similar to that on the stoichiometric surface, and SH is also adsorbed at the Cu_{SUB}–Cu_{SUB} bridge site with S-down mode, two Cu—S bonds (2.225 and 2.401 Å) are formed, the adsorption free energy is 208.6 kJ mol^{-1}.

3.2. H_2S adsorption

In the case of H_2S adsorption, taking two types of initial configurations into consideration, one is that the plane of H_2S is perpendicular to the surface via S interaction with the surface; the other is that the plane of H_2S is parallel to the surface via S interaction with the surface.

3.2.1. On the stoichiometric surface

Interestingly, our results show that after optimization, H_2S initially adsorbed at the Cu_{SUB}–Cu_{SUB} bridge and O_{SUF} sites with the plane of H_2S parallel to the surface is spontaneously dissociated into SH and H species, suggesting that H_2S is the dissociative adsorption; SH_b and H_a species are adsorbed at the Cu_{SUB} and O_{SUF} sites, respectively, as shown in Fig. 2(a).

Except for above initial configurations, other initial adsorption configurations are all converted to that with H_2S adsorbed at Cu_{SUB}

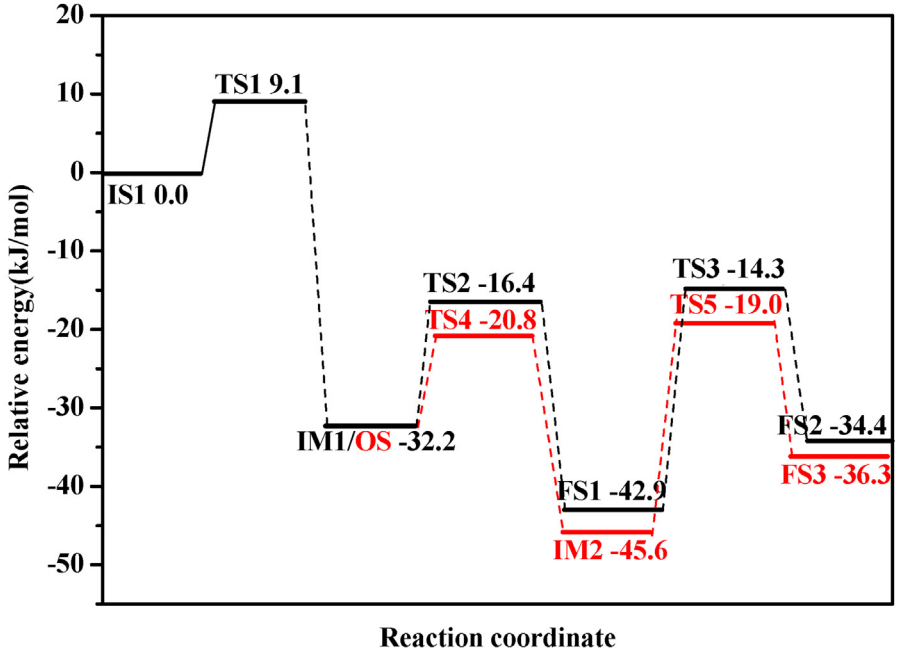

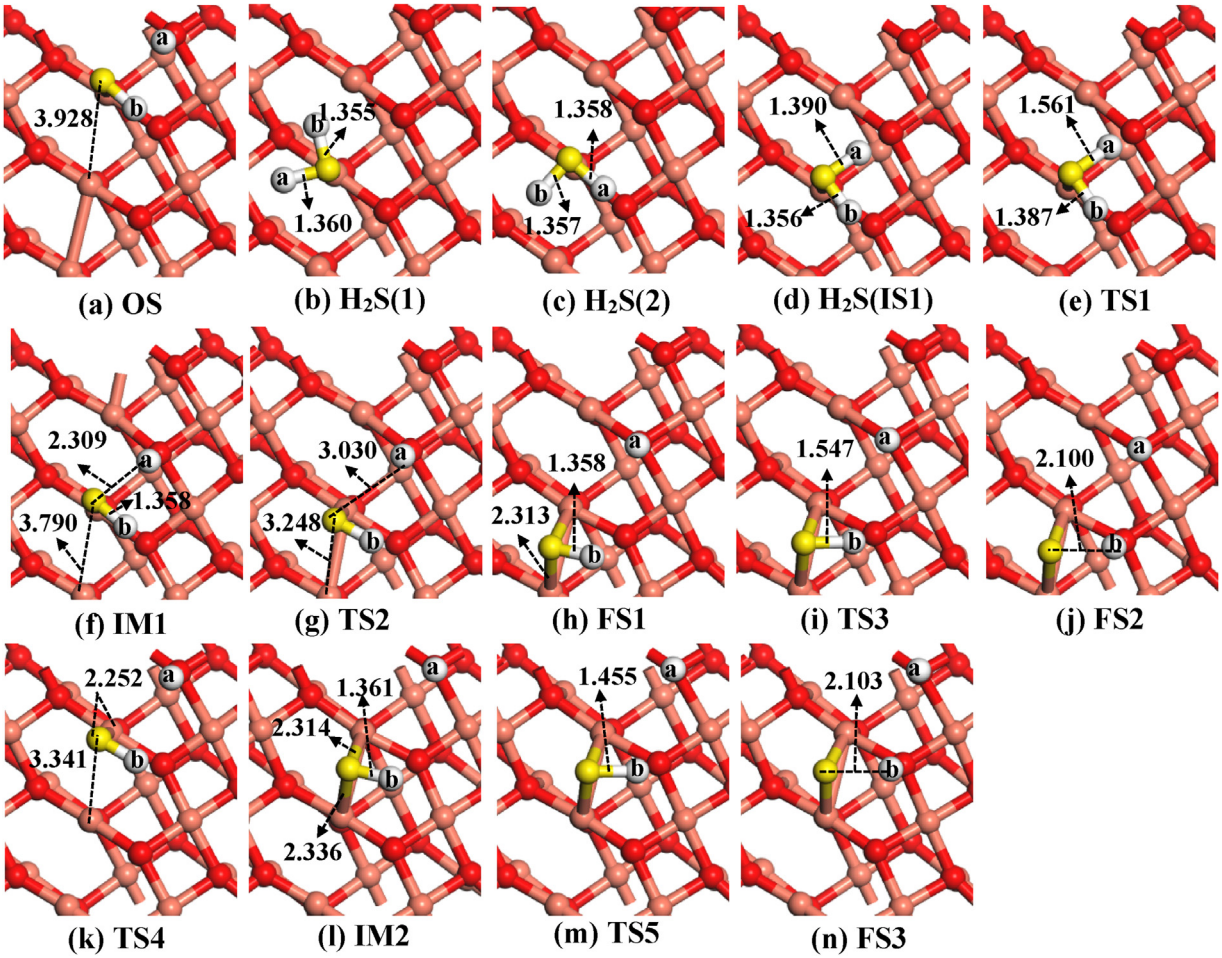

Fig. 2. The dissociative adsorption configuration (OS) and three optimized stable configurations of H_2S species adsorbed at Cu_{SUB} site, as well as the potential energy profiles of molecular adsorption H_2S dissociation at Cu_{SUB} site (black line) and the dissociation of the dissociative adsorption H_2S (red line) into the final products S and H species together with the initial states (ISs), transition states (TSs), final states (FSs) and intermediates (IMs) on the stoichiometric CuO(111) surface. Bond lengths are in Å. See Fig. 1 for color coding. (For interpretation of the references to colour in this figure legend, the reader is referred to the web version of this article.)

site via S atom or that H_2S is far away from the surface. Thus, three stable configurations of $H_2S(1)$, $H_2S(2)$ and $H_2S(IS1)$, as shown in Fig. 2(b)–(d), have been obtained, H_2S are all adsorbed at Cu_{SUB} site via S atom. In $H_2S(1)$, one H atom points to O_{SUB} site, the other is inclined to Cu_{SUF} site; In $H_2S(2)$, two H atoms are inclined to O_{SUB} and O_{SUF} sites, respectively; In $H_2S(IS1)$, two H atoms all point to different O_{SUF} sites. The adsorption free energies of $H_2S(1)$, $H_2S(2)$ and $H_2S(IS1)$ are 88.3, 95.7 and 96.0 kJ mol^{-1}, respectively. Thus, $H_2S(IS1)$ is the most stable adsorption configuration, which is selected to be the initial state of H_2S dissociation.

In $H_2S(IS1)$, one Cu_{SUB}—S bond (2.126 Å) is formed, and the H_a—S bond of H_2S (1.390 Å) is greatly elongated compared to that in gas phase H_2S molecule (1.352 Å), the H_a—S bond elongation is in favor of H_2S activation and dissociation.

Thus, H_2S dominantly exists in the form of dissociative adsorption leading to SH and H species on the stoichiometric surface. Meanwhile, a small quantity of molecular adsorption H_2S at Cu_{SUB} site also exist, the adsorption promotes H—S bond activation, and contributes to H_2S dissociation.

3.2.2. On the reduced surface

In the case of H_2S adsorption on the reduced surface, eight types of initial adsorption configurations are considered, as presented in Fig. 3(a)–(h), which is named as IC-x, (a) H_2S lies flatly at Cu^1 site with S atom; (b) H_2S lies over Cu^2 site via S atom; (c) H_2S lies over $O_{vacancy}$ site via S atom; (d) H_2S lies over Cu^1–$O_{vacancy}$ bridge site via S atom; (e) H_2S lies over Cu^1–Cu^2 bridge site via S atom; (f) H_2S lies over Cu^2–Cu^4 bridge site via S atom. (g) H_2S lies flatly over Cu^1–$O_{vacancy}$ bridge site via S and H atoms; (h) H_2S lies over $O_{vacancy}$ site via S and H atoms. The optimized configurations are shown in Fig. 3(i)–(n).

Except for IC-1, IC-6, IC-7 and IC-8 modes, H_2S in other initial configurations are spontaneously dissociated into SH and H species. The initial structures of IC-2, IC-4 and IC-5 are converted to the optimized structures OS-1, OS-2 and OS-1, respectively; the initial structure IC-3 is converted to OS-3. In OS-1 and OS-2, the SH group and H atom are adsorbed at the Cu^1–Cu^2 bridge and O_{SUF} sites, respectively, where H_b atom is pointed to $O_{vacancy}$ and O_{SUB} sites, respectively. In OS-3, the SH group and H atom are adsorbed at the $O_{vacancy}$ and Cu_{SUB}–Cu_{SUB} bridge sites, respectively. In OS-1 ~ OS-3, the rather long distances between H_a and S atom (2.912, 2.811, and 2.941 Å) indicate that the H_a—S bond of H_2S is completely broken, which is typical of dissociative adsorption modes.

On the other hand, the initial IC-1 mode is optimized to OS-4 with H_2S adsorbed at Cu^1 site with an adsorption free energy of 143.4 kJ mol^{-1}, the H_a—S bond of H_2S (1.382 Å) is significantly stretched relative to that in gas phase H_2S (1.352 Å), which contributes to H_2S dissociation. Moreover, the initial adsorption structures of IC-6 and IC-7 are all converted to OS-5, the H—S bond lengths both are 1.361 Å, where two H—S bond is slightly changed compared to that in the free H_2S molecule (1.352 Å), the adsorption free energy is 141.9 kJ mol^{-1}. Meanwhile, the initial structures of IC-8 is converted to OS-6 with an adsorption free energy of 136.8 kJ mol^{-1}, the H—S bond lengths are 1.359 and 1.379 Å, respectively. The adsorption free energies of above three structures are in the following order: OS–4 > OS–6 > OS-5, suggesting that Cu^1 site is the most stable site for H_2S molecular adsorption on the reduced surface, which is selected as the initial state of H_2S dissociation reaction, as shown in Fig. 4.

Above results indicate that H_2S exists in the form of molecular adsorption and dissociative adsorption on the reduced CuO(111) surface, and the latter is the dominant pathway for H_2S dissociation into H atom and SH group.

Table 1
The microscopic parameters of molecular adsorption H_2S on different CuO(111) surfaces.

Parameters and charge	Stoichiometric	Reduced	Sulfurized
	H_2S (IS1)	H_2S (IS2)	$H_2S + S_p$ (IS3)
$d_{S\text{-}Cu}$ (Å)[a]	2.413	2.275	2.408
$d_{Ha\text{-}S}$ (Å)[b]	1.390	1.382	1.362
Charge of H (e)	0.267	0.272	0.227
	0.220	0.216	0.232
Charge of S (e)	−0.182	−0.111	-0.122 (H_2S)
			-0.063 (S_p)
Charge of H_2S (e)	0.305	0.377	0.337
G_{ads} (kJ mol^{-1})	96.0	143.4	107.0

[a] $d_{S\text{-}Cu}$ (Å) is the distance between S atom and its nearby Cu site.
[b] $d_{Ha\text{-}S}$ (Å) is the H_a—S bond length.

3.2.3. On the sulfurized surface

As mentioned above, on the stoichiometric surface, Cu_{SUB} is the stable site for H_2S molecular adsorption, and H_2S is the dissociative adsorption when initially adsorbed at the Cu_{SUB}–Cu_{SUB} bridge and O_{SUF} sites with the plane of H_2S parallel to the surface via S atom binding to the surface, thus, in this section, we only test three initial adsorption configurations on the sulfurized surface, in which H_2S is adsorbed at the Cu_{SUB}–Cu_{SUB} bridge, Cu_{SUB} and O_{SUF} sites via S atom with the plane of H_2S parallel to the surface, respectively.

H_2S initially adsorbed at O_{SUF} site is the dissociative adsorption, as shown in Fig. 5(a), in which SH and H species are all adsorbed at two O_{SUF} sites. Then, H_2S initially adsorbed at the Cu_{SUB}–Cu_{SUB} bridge and Cu_{SUB} sites are all converted to the optimized structure, as shown in Fig. 5(b), H_2S is parallel to the surface with S adsorbed at Cu_{SUB} site with the adsorption free energy of 107.0 kJ mol^{-1}.

3.2.4. Brief summary

On the basis of above results, we can obtain that H_2S mainly exists in the form of dissociative adsorption on different CuO(111) surfaces, which can spontaneously form SH and H species. Meanwhile, a small quantity of H_2S also exists in the form of molecular adsorption, and H_2S adsorption promotes the H—S bond activation, which is in favor of H_2S dissociation.

By comparing the adsorption of H_2S on the stoichiometric and sulfurized surface, we can found that the Cu_{SUB}–Cu_{SUB} bridge site fails to contribute to the spontaneous dissociation of H_2S on the sulfurized surface, while H_2S is the dissociative adsorption when initially adsorbed at Cu_{SUB}–Cu_{SUB} bridge site on the stoichiometric surface, suggesting that the existence of S atom on the stoichiometric surface weakens the activity toward H_2S dissociation.

On the other hand, for molecular adsorption H_2S, as shown in Fig. 5(b), the corresponding adsorption free energy on the sulfurized surface (107.0 kJ mol^{-1}) is larger by 11.0 kJ mol^{-1} than that on the stoichiometric surface (96.0 kJ mol^{-1}), suggesting that the existence of surface S atom slightly promotes the strength of H_2S adsorption on CuO(111) surface. As listed in Table 1, compared to the stoichiometric surface, the charge of H_2S is increased by 0.032 e on the sulfurized surface; these results well explain why the surface S atom can enhance the strength of H_2S adsorption. However, the H_a—S bond of H_2S (1.362 Å) on the sulfurized surface is significantly shorter than that on the stoichiometric surface (1.390 Å), and there isn't difference from that in the gas phase H_2S (1.352 Å), suggesting the existence of sulfur atom can suppress the H—S bond activation of H_2S. In the case of reduced surface, the corresponding adsorption free energy of H_2S is 143.4 kJ mol^{-1}, which is larger by 47.4 and 36.4 kJ mol^{-1} than those on the stoichiometric and sulfurized surface, suggesting that the surface reduction enhances the adsorption strength of H_2S on CuO(111) surface. As listed in Table 1, compared to the stoichiometric surface, the charge of H_2S is increased by 0.072 e, and the distance between S and nearby Cu atom is shortened

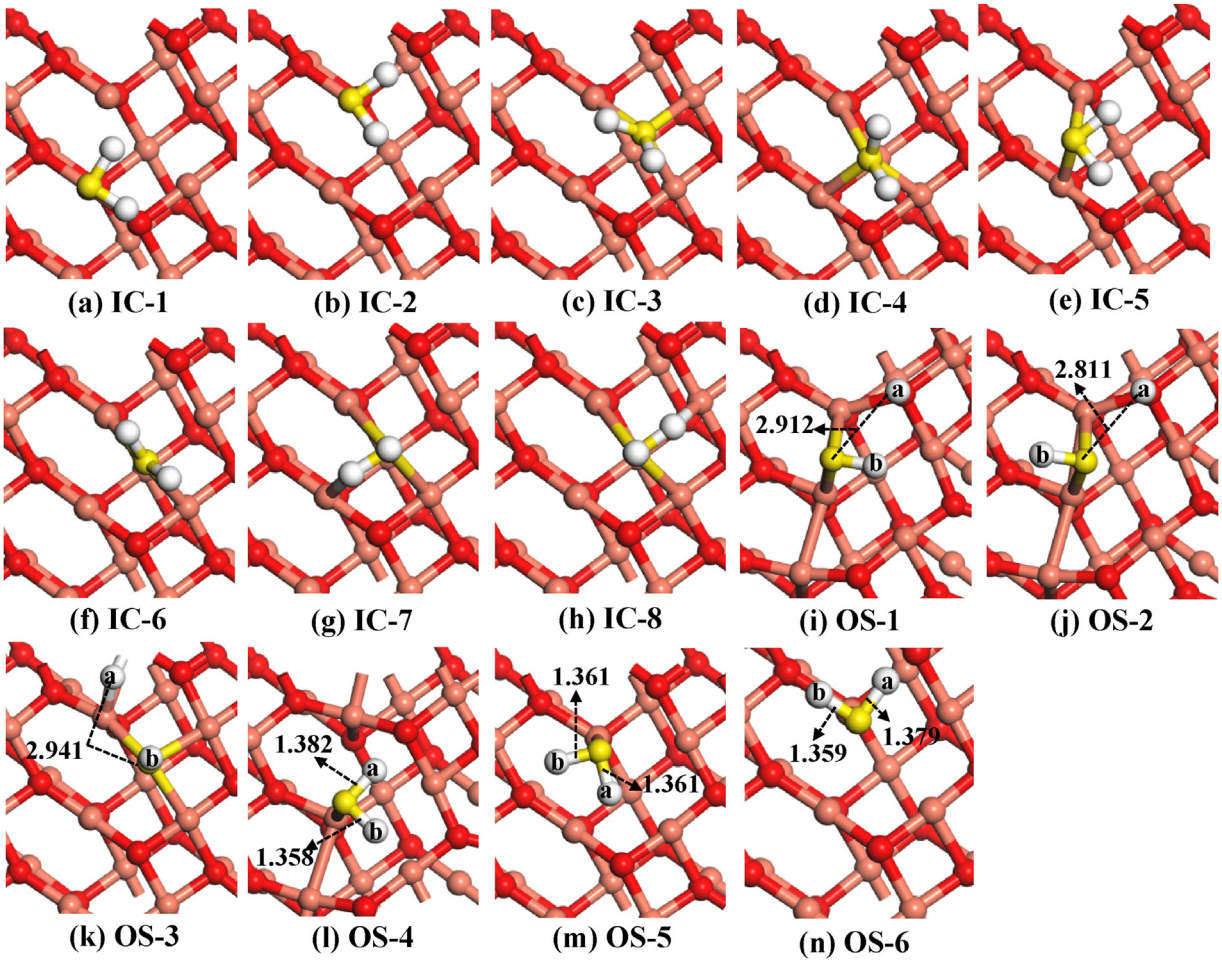

Fig. 3. All possible initial configurations (ICs) and the corresponding optimized structures (OSs) of H_2S adsorbed on the reduced CuO(111) surface. Bond lengths are in Å. See Fig. 1 for color coding.(For interpretation of the references to colour in this figure legend, the reader is referred to the web version of this article.)

Table 2
The calculated results for gaseous and adsorbed H_2S: antisymmetric stretching frequency (υ_{asym}), symmetric stretching frequency (υ_{sym}), H-S-H bending frequency (υ_{bend}), together with those for gaseous and adsorbed SH group: stretching frequency (υ_{asym}), Cu-S-H bending frequency (υ_{bend}).

	Species	Vibrational frequencies/cm^{-1}		
		υ_{asym}	υ_{sym}	υ_{bend}
H_2S	Stoichiometric	2595	2210	1184
	Reduced (Cu^1)	2573	2300	1151
	Sulfurized	2557	2518	1186
	Gas phase	2678	2660	1191
SH	Stoichiometric	2591		590
	Reduced	2545		596
	Sulfurized	2590		623
	Gas phase	2632		

by 0.138 Å on the reduced surface; moreover, H_2S is the dissociative adsorption for the first dehydrogenation step, which agrees with the previous studies about H_2S interaction with the reduced ZnO(10-10) surface [21]. In addition, on the reduced Cu_2O(111) surface, SH species can be also spontaneously formed due to H_2S dissociative adsorption [18].

3.3. Vibrational frequencies

Table 2 presents the calculated vibrational frequencies of the adsorbed SH and H_2S species on different CuO(111) surfaces, we can clearly find that the symmetric and anti-symmetric of H—S stretching frequencies of H_2S, as well as the H—S stretching frequency of adsorbed SH significantly reduce upon adsorption on the different surfaces. On the other hand, the red-shift of the H—S stretching frequencies for H_2S adsorbed on different surfaces indicate that the strength of H—S bond decreases, which give the reasons of H—S bond elongation involved in Section 3.2.

3.4. Molecular adsorption H_2S dissociation

3.4.1. The dissociation of molecular adsorption H_2S

The dissociation mechanism of H_2S involves the two sequential dehydrogenation step [39–42], one is that $H_2S \rightarrow SH + H$, and the other is that $SH \rightarrow S + H$.

3.4.1.1. Stoichiometric surface. In the first step of H_2S dissociation, the most stable adsorption configuration H_2S(IS1) is chosen as the initial state IS1, as shown in Fig. 2(d), which contributes to the formation of H_a and SH_b species due to the H_a—S bond cleavage. On the other hand, since SH and H species prefer to adsorb at the Cu_{SUB}–Cu_{SUB} bridge and O_{SUF} sites, respectively, the optimized configuration for the initial co-adsorption, H_a and SH_b adsorbed at the O_{SUF} and Cu_{SUB}–Cu_{SUB} bridge sites, is selected as the final state (FS1) for the first step of H_2S dissociation.

The potential energy profiles for the dissociation of H_2S together with the initial states (ISs), intermediates (IMs), transition states (TSs) and final states (FSs) at the temperature of 475 K are presented

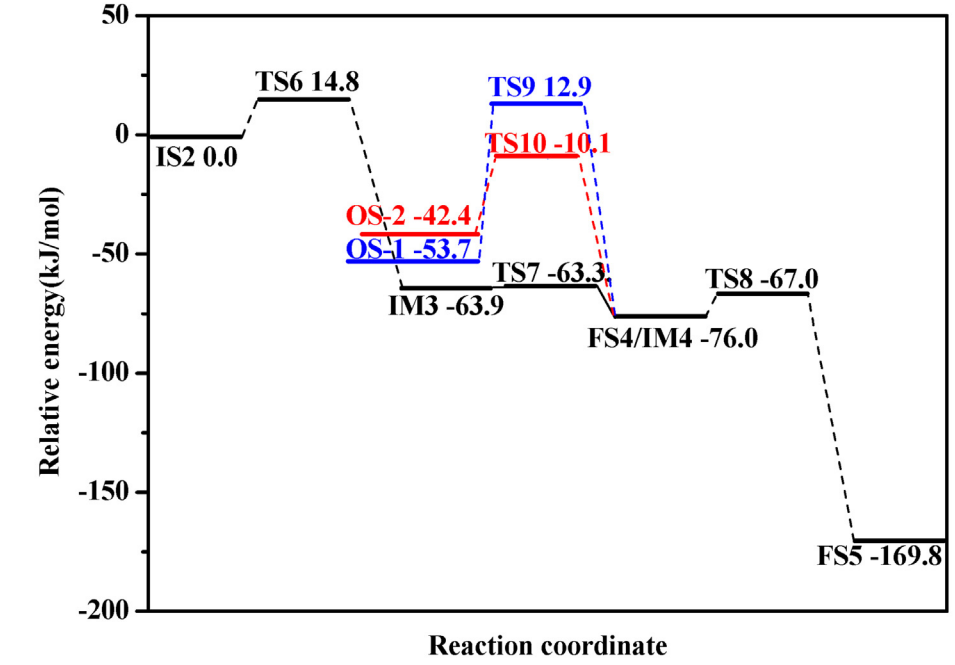

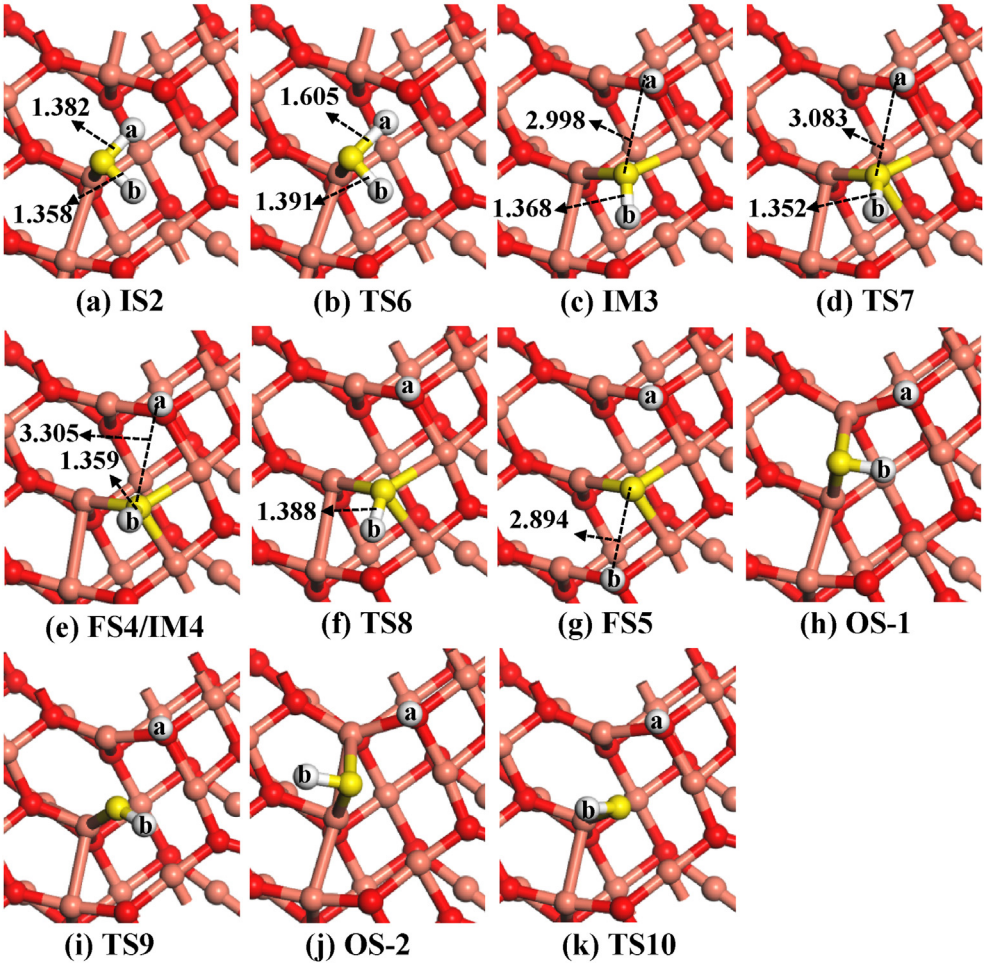

Fig. 4. Potential energy profiles for the dehydrogenation of molecular adsorption H_2S at Cu^1 site on the reduced surface leading to the final products S and H species adsorbed at $O_{vacancy}$ and O_{SUF} sites, respectively (black line), as well as the dehydrogenation of dissociative adsorption H_2S of OS1 (blue line), OS2 (red line) in Fig. 3 together with the initial states (ISs), transition states (TSs), final states (FSs) and intermediates (IMs). Bond lengths are in Å. See Fig. 1 for color coding. (For interpretation of the references to colour in this figure legend, the reader is referred to the web version of this article.)

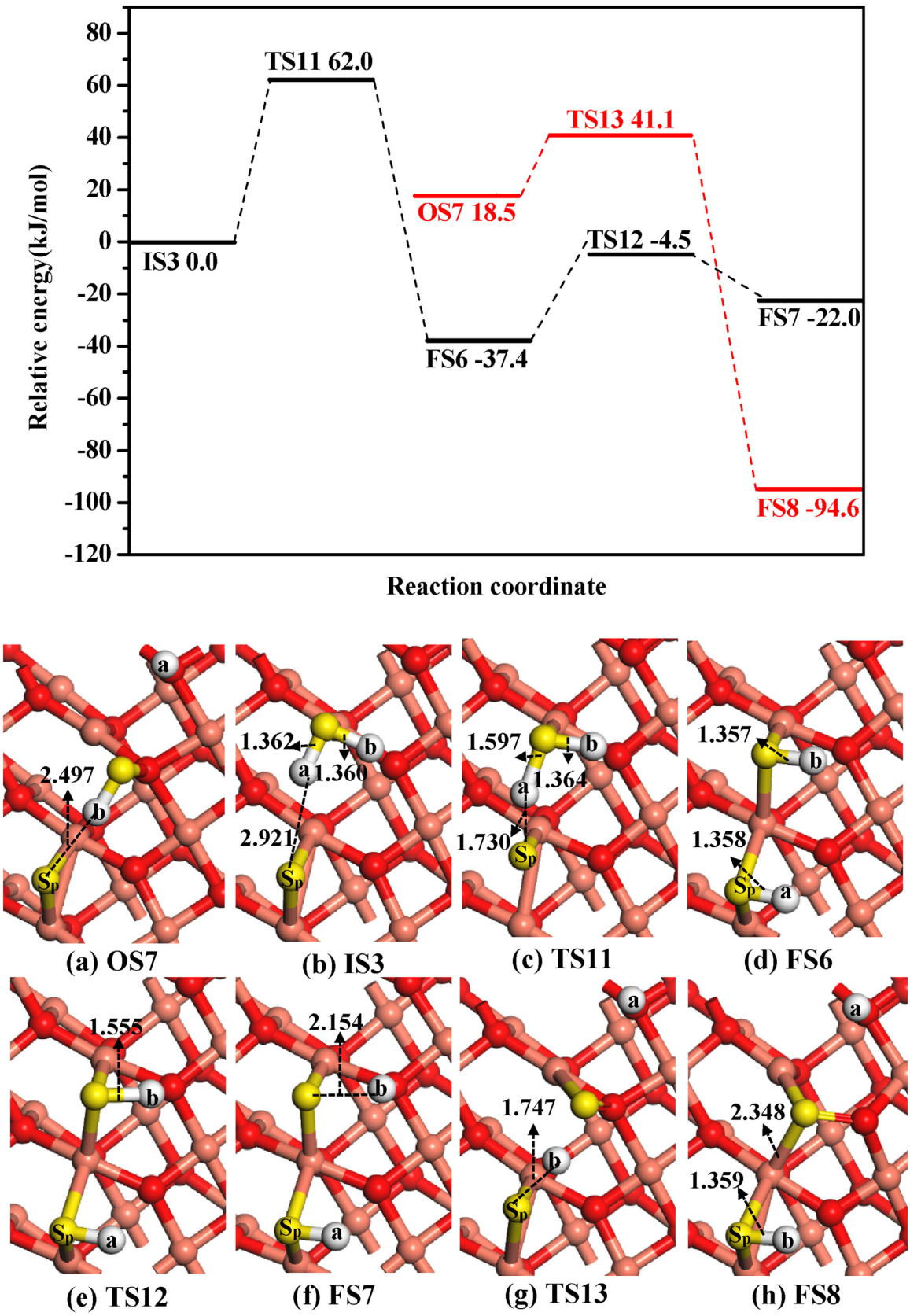

Fig. 5. Potential energy profiles for the dehydrogenation of chemisorption H_2S at Cu_{SUB} site on the sulfurized surface leading to the final products S and H species (black line), as well as the dehydrogenation of dissociative adsorption H_2S of OS7 (red line) together with the initial states (ISs), transition states (TSs), final states (FSs) and intermediates (IMs). Bond lengths are in Å. See Fig. 1 for color coding. (For interpretation of the references to colour in this figure legend, the reader is referred to the web version of this article.)

in Fig. 2. We can see that the initial state H_2S(IS1) can form the final states (FS1) via an intermediate (IM1). Firstly, H_2S breaks its H_a—S bond to form IM1 via TS1, this elementary reaction is exothermic by 32.2 kJ mol^{-1} with a small activation free energy of 9.1 kJ mol^{-1}, which is far lower than the adsorption free energy (96.0 kJ mol^{-1}) of H_2S on the stoichiometric surface, namely, molecular adsorption H_2S prefers to dissociate into SH and H species rather than its desorption. In TS1, the activated H_a—S bond is elongated to 1.561 Å from 1.390 Å in IS1, further elongated to 2.309 Å in IM1, suggesting that H—S bond is completely broken in IM1. In IM1, H_a atom is adsorbed at a nearby O_{SUF} site, and SH_b group still adsorbs at Cu_{SUB} site; subsequently, IM1 can form FS1 via TS2 with the transfer of SH_b from Cu_{SUB} to Cu_{SUB}–Cu_{SUB} bridge site, this elementary reaction has also a small activation free energy of 15.8 kJ mol^{-1}, and it is exothermic by 10.7 kJ mol^{-1}.

3.4.1.2. Reduced surface. The initial dissociation step of molecular adsorption H_2S at Cu^1 site has been considered. We can see from Figs. 3 and 4, the structure OS-4 and the co-adsorption configuration of SH and H species are selected as the initial state (IS2) and the final state (FS4), respectively, to gain insight into the first dehydrogenation step of H_2S on the reduced surface.

Fig. 4 presents the potential energy profiles for the dissociation of H_2S on the reduced surface and the corresponding structures at the temperature of 475 K. Through one intermediate (IM3) and two transition states (TS6, TS7), the co-adsorbed SH_b and H_a species (FS4) can be formed from the initial structure (IS2). Starting from H_2S adsorbed at Cu^1 site, where the H_a—S bond length is 1.382 Å; subsequently, H_2S dissociates into H_a atom adsorbed at the adjacent O_{SUF} site and SH_b group filled into the $O_{vacancy}$ site; In IM3, the H—S bond is completely broken. The H_a—S bond stretching is the dominant reaction, which is extended 1.382 Å (IS2) → 1.605 Å (TS6) → 2.998 Å (IM3) → 3.083 Å (TS7) → 3.305 Å (FS4). This elementary step has an activation free energy of 14.8 kJ mol^{-1}, and it is exothermic by 76.0 kJ mol^{-1}.

3.4.1.3. Sulfurized surface. The most favorable configuration of H_2S parallel to the surface with S adsorbed at Cu_{SUB} site is selected as the initial state (IS3) to investigate the initial dissociation of H_2S on the sulfurized surface, as shown in Fig. 5, the cleavage of H_a—S bond in IS3 can form the co-adsorbed SH_b and H_a species (FS6) via a transition state (TS11), in which H_a atom is migrated to S_p site to form SH_b and S_pH_a species adsorbed at different Cu_{SUB}–Cu_{SUB} bridge sites through S atom, respectively. This elementary reaction is strongly exothermic by 37.4 kJ mol^{-1} with the activation free energy of 62.0 kJ mol^{-1}. In TS11, the dissociating H_a–S bond distance is 1.597 Å; the H_a—S_p bond length is 1.730 Å.

3.4.2. The dissociation of SH

Two types of SH dissociation are discussed, one is the dissociation of SH from H_2S dissociation, the other is the dissociation of SH from H_2S dissociative adsorption.

3.4.2.1. SH dissociation from molecular adsorption H_2S. For the stoichiometric surface, FS1 is considered as the initial state for SH dissociation from molecular adsorption H_2S. In the case of the final state, its initial co-adsorption configuration is that two H and one S atom are adsorbed at two adjacent O_{SUF} and the Cu_{SUB}–Cu_{SUB} bridge sites, respectively, and the optimized structure is chosen as the final state (FS2), as shown in Fig. 2(j). Starting from FS1, SH_b breaks its H_b—S bond to form FS2 via TS3, this elementary reaction is slightly endothermic by 8.5 kJ mol^{-1}, and it has an activation free energy of 28.6 kJ mol^{-1}; in TS3, H atom of SH_b group is inclined to the adjacent O_{SUF} site, and the activated H_b—S bond is elongated to 1.547 Å from 1.358 Å in FS1, and finally elongated to 2.100 Å in FS2. In FS2, H atoms are adsorbed at two O_{SUF} sites, respectively; S atom is still adsorbed at the Cu_{SUB}–Cu_{SUB} bridge site.

On the reduced surface, FS4 in Fig. 4(e) is selected as the initial state to investigate SH dissociation. The H_b—S bond gradually breaks along with the elongation of H_b—S bond from 1.359 Å (FS4) to 1.388 Å (TS8), and eventually forms FS5, in which S is filled into $O_{vacancy}$ site, while both H_a and H_b atoms are adsorbed at two O_{SUF} sites. This elementary step overcomes a small activation free energy of 9.0 kJ mol^{-1}, which is strongly exothermic by 93.8 kJ mol^{-1}, suggesting that S and H species are the favorable products both thermodynamically and kinetically.

On the sulfurized surface, the H_b—S bond cleavage of SH_b is investigated. As shown in Fig. 5, along with the migration of H_b atom from S atom to surface O_{SUF} atom, FS6 goes through a transition state (TS12) to form the final product (FS7). The H_b—S bond is elongated from 1.357 Å in FS6 to 1.555 Å (TS12), and finally stretched to 2.154 Å in FS7. The corresponding activation free energy is 32.9 kJ mol^{-1}, it is endothermic by 15.4 kJ mol^{-1}.

3.4.2.2. SH dissociation from dissociative adsorption H_2S. On the stoichiometric surface, H_2S adsorbed at the Cu_{SUB}–Cu_{SUB} bridge and O_{SUF} sites is the dissociative adsorption, which lead to the formation of SH and H species, as shown in Fig. 2(a); subsequently, the adsorbed SH_b can further dissociate into S and H atoms. Thus, we investigate SH dissociation from the dissociative adsorption H_2S. As shown in Fig. 2, the dissociative adsorption structure OS is similar to the intermediate IM1. Similar to the dissociation of IM1, the initial state OS can form the final states (FS3) via an intermediate (IM2) and two transition states TS4 and TS5, whose structure is also similar with TS2 and TS3, respectively. These two elementary reactions have the activation free energies of 11.4 and 26.6 kJ mol^{-1} with the corresponding reaction free energies of −13.4 and 9.3 kJ mol^{-1}, respectively, and these values are also close to those for the dissociation of intermediate IM1 into S and H atoms.

On the reduced surface, three dissociative adsorption configurations also exist, as listed in Fig. 3(i)–(k). However, H_a atom in OS-3 adsorbed at the Cu_{SUB}–Cu_{SUB} site is not the favorable adsorption site for H adsorption, it is more likely to be converted into the configurations OS-1 or OS-2, thus, we neglect the dissociative adsorption structures OS-3 for the investigation of SH dissociation from the dissociative adsorption H_2S. Consequently, the configurations OS-1 and OS-2 are selected as the initial states. Our results indicate that OS-1 and OS-2, as shown in Fig. 4, can form the same intermediate (IM4) via the transition states TS9 and TS10, respectively, and both elementary reactions have the activation free energies of 66.6 and 32.3 kJ mol^{-1} with the reaction free energies of −22.3 and −33.6 kJ mol^{-1}, respectively; then, IM4 can form the final states (FS5) via TS8, which is the same with the dissociation pathway of SH species from molecular adsorption H_2S dissociation.

On the sulfurized surface, the dissociative adsorption structure OS7, as shown in Fig. 5(a), is taken as the initial state; then, the initial co-adsorption configuration is that S and two H atom are adsorbed at the Cu_{SUB}–Cu_{SUB} bridge, O_{SUF} and S_p sites, respectively, the corresponding optimized configuration is regarded as the final state (FS8) for the dissociation of SH from dissociative adsorption H_2S. As shown in Fig. 5, the dissociative adsorption structure OS7 can form the final states (FS8) via the transition state TS13, this elementary step is highly exothermic by 113.1 kJ mol^{-1} with an activation free energy of 22.6 kJ mol^{-1}.

3.4.3. Brief summary

Above results indicate that H_2S mainly exists in the form of dissociative adsorption on different CuO(111) surfaces, which contribute to the formation of SH and H species, meanwhile, molecular adsorption H_2S also exists on different surfaces, which can dissociate into SH and H due to the H—S bond activation.

For the stoichiometric surface, molecular adsorption H_2S exists at Cu_{SUB} site, the first dissociation step of molecular adsorption H_2S to SH and H species only requires a small activation free energy of 9.1 kJ mol^{-1}, namely, SH and H species can be easily formed on the stoichiometric CuO(111) surface, which not only come from the dissociative adsorption of H_2S, but also from the dissociation of molecular adsorption H_2S. Subsequently, SH dissociates into S and H species, the activation free energy (28.6 kJ mol^{-1}) is higher than the first step of H_2S dissociation, however, the first dehydrogenation step of molecular adsorption H_2S is strongly exothermic (42.9 kJ mol^{-1}), which is far more than the required activation free energy (28.6 kJ mol^{-1}) for the second dehydrogenation step. Thus, SH also easily dissociate into S and H species. Our calculated activation free energies of the first (9.1 kJ mol^{-1}) and second (28.6 kJ mol^{-1}) dehydrogenation steps are consistent with the previous studies about H_2S dissociation on the stoichiometric CuO(111) surface at 0 K with the values of 2.4 and 23.1 kJ mol^{-1}, respectively [15], suggesting that the change of temperature has little effect on the activation free energy. On the other hand, only the dissociation of molecular adsorption H_2S has been investigated in the previous studies [15], the dissociative adsorption of H_2S have not been examined; however, our results show that the dissociative adsorption dominantly contributes to the first dissociation step of H_2S into SH and H species, which is quite different from the previous studies [15].

On the reduced surface, the dissociation of molecular adsorption H_2S at Cu^1 site exists, as presented in Fig. 4, the low activation free energies (14.8 kJ mol^{-1}) and strongly exothermic (76.0 kJ mol^{-1}) of the first dehydrogenation step indicate that this reaction is likely to occur kinetically and thermodynamically, namely, SH species can be easily formed on the reduced surface. Subsequently, the dissociation of SH occurs, which requires a lower activation free energies (9.0 kJ mol^{-1}) relative to the first dehydrogenation step (14.8 kJ mol^{-1}) with the strongly exothermic (93.8 kJ mol^{-1}).

On the sulfurized surface, as presented in Fig. 5, the activation free energy of H_2S dissociation at Cu_{SUB} site in the first step is 62.0 kJ mol^{-1}, which is far less than the adsorption free energy (107.0 kJ mol^{-1}) of H_2S at Cu_{SUB} site, suggesting that SH can be formed by H_2S dissociation. Meanwhile, the first step of H_2S dissociation is exothermic by 37.4 kJ mol^{-1}, which can promote the second decomposition of H_2S.

3.5. General discussion

As mentioned above, H_2S adsorption and dissociation into the final products S and H species on three types of CuO(111) surfaces have been systematically examined. We can clearly find that H_2S dominantly exists in the form of dissociative adsorption on the stoichiometric, reduced and sulfurized surfaces leading to the formation of SH and H species. Our results agree well with the previous experimental studies, which have proposed that the initial step of H_2S is the dissociative adsorption on CuO surface, then, the sulphide species is formed by an O/S replacement mechanism in the case of high concentration H_2S [16]. Thus, based on the reaction process of $CuO + H_2S \rightarrow CuS + H_2O$, the predominant (111) surface of CuO is considered as a promising material of gas sensor [11,29].

On the other hand, when H_2S initially adsorbed at the Cu_{SUB}–Cu_{SUB} bridge site on the stoichiometric surfaces is dissociative adsorption, while H_2S exists in the form of molecular adsorption on the sulfurized surface, suggesting that the existence of S atom adsorbed at the Cu_{SUB}–Cu_{SUB} bridge site decreases the number of the active center toward H_2S dissociation, thereby weakens the catalytic activity of stoichiometric surface toward H_2S initial dehydrogenation. In addition, previous studies have indicated that the strongly adsorbed S species from H_2S dissociation on Ni(100) surface block the active sites of CO, and thereby make CO redistribute into several desorption states [43].

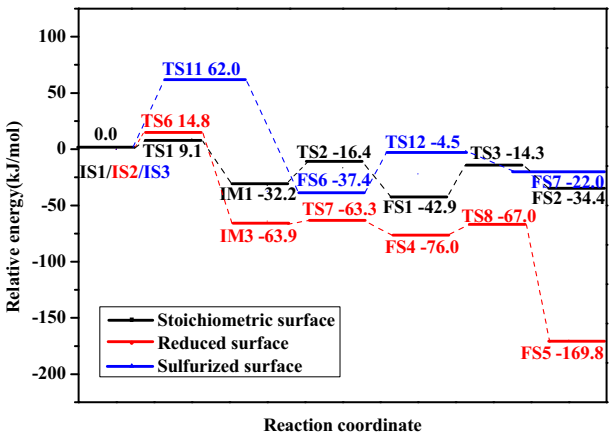

Fig. 6. Schematic potential energy diagrams for the dissociation of molecular adsorption H_2S leading to S and H species on the stoichiometric surface (black line), the reduced surface (red line), and the sulfurized CuO(111) surface (blue line), respectively. (For interpretation of the references to colour in this figure legend, the reader is referred to the web version of this article.)

Since SH and H species can be easily formed on different CuO(111) surface from the first step of H_2S dehydrogenation, once SH species is formed, S species are inevitably formed since the first step of H_2S dehydrogenation is a strong exothermic reaction, which can provide the needed energy for the subsequent dissociation SH species. Meanwhile, a small quantity of molecular adsorption H_2S also exists on these three surfaces. Thus, we further discuss the differences of molecular adsorption H_2S dissociation and dissociative adsorption H_2S leading to S and H species on the stoichiometric, reduced and sulfurized CuO(111) surfaces, the corresponding simplified potential energy profiles is shown in Fig. 6.

According to Fig. 6, the whole dehydrogenation process from the adsorbed H_2S molecule to the end-product S and H species is exothermic on these three surfaces, suggesting that the dissociation is favorable in consideration of thermodynamics. On the other hand, taking the kinetics into consideration, the highest activation free energy and reaction free energy on the stoichiometric surfaces are 9.1 and −34.4 kJ mol^{-1}, respectively, whereas those on the reduced surface are 14.8 and −169.8 kJ mol^{-1}, respectively, suggesting that S and H species can be easily generated from H_2S dissociation on the stoichiometric CuO(111) surface in the view of kinetics compared to that on the reduced surface. However, in the case of the sulfurized surface, the highest activation free energy and free energy change of H_2S dissociation are 62.0 and −22.0 kJ mol^{-1}, respectively, this dissociation process has the largest activation free energy, and releases the least heat compared to that on the stoichiometric and reduced surfaces, indicating that the sulfurized surface is unfavorable for H_2S dissociation both thermodynamically and kinetically compared to that on the stoichiometric and reduced surfaces, namely, the existence of sulfur atom significantly reduces the catalytic activities of CuO(111) surface toward H_2S dissociation, indicating that CuO(111) surface is poisoned by S element. Moreover, previous studies about CO adsorption and dissociation on the sulfurized Fe(100) surface have suggested that the dissociation of CO is favorable in consideration of thermodynamics on the S-free surface, whereas it becomes unfavorable due to the existence of S element, in this case, sulfur also acts as a poison [44]. Further, for the sulfurized Cu_2O(111) surface, the presence of surface S atom resists the process of H—S bond-breaking, which also have negative effects on H_2S dissociation [18].

In order to provide a deep explanation for structure properties of the different CuO(111) surfaces, the projected density of states

Table 3
Average energy (ε_d) and width (W_d) of the *d*-band for the surface Cu atoms on different CuO(111) surface.

Surface	ε_d (eV)	W_d (eV)
Stoichiometric	−2.58	10.42
Reduced	−2.61	10.49
Sulfurized	−2.71	11.07

(pDOS) and *d*-band analysis are employed in our calculation, as listed in Table 3, the detailed descriptions are shown in Part 5 of the Supplementary Material. Generally, a more reactive metal on the surface of catalysts corresponds to the closer the *d*-band center to the Fermi level and the lower value of the bandwidth [45].

For a certain reaction, the activation free energy is extremely related to the electronic structure of the atoms on the catalyst surface and its reaction route [46]. Meanwhile, H_2S dissociation on different CuO(111) surfaces has the similar reaction route, as a result, a clear understanding about the effect of electronic structure on the activation free energy is of great importance. Thus, the electronic structure analysis is adopted to gain insight into the difference in catalytic activity for different CuO(111) surfaces. Since H_2S always interacts with Cu atom via S atom on the different CuO(111) surfaces, the projected densities of states (pDOS) of Cu *d*-band (see Fig. 7) on the different CuO(111) surfaces are calculated in this study, in which only the surface Cu atoms is considered in the calculations. As presented in Fig. 7, the *d*-band center of sulfurized surface is away from the Fermi level compared to that on the stoichiometric and reduced surfaces; the *d*-band energy of the stoichiometric surface is closer to the Fermi level. On the other hand, as listed in Table 3, the largest bandwidth (11.07 eV) on the sulfurized leads to a less reactive surface Cu atom, whereas the stoichiometric surface has the lowest bandwidth (10.42 eV), which contributes to the more reactive surface Cu atoms. Consequently, the catalytic activity of Cu atoms on these three surfaces follows the order: Stoichiometric > Reduced > Sulfurized surface. This result agrees with the kinetic result of H_2S dissociation.

Further, as presented in Fig. 6, the highest activation free energies of H_2S dissociation on these three CuO(111) surfaces all attribute to the first dehydrogenation step of H_2S; as a result, the degree of H_2S activation plays a crucial role in H_2S dissociation. Thus, we also compare the bond length of H_a–S in the first step of H_2S dehydrogenation on these three surfaces, in which the longer bond length represents the higher degree of H_2S activation. As shown in Table 1, H_2S adsorbed on the stoichiometric surface has the largest bond length (1.390 Å) compared to that on the reduced (1.382 Å) and sulfurized surfaces (1.362 Å), indicating that H_2S adsorbed on the stoichiometric surface acquires the greatest H—S bond activation degree, which is in line with the lowest activation free energy (9.1 kJ mol^{-1}). On the contrary, H_2S adsorbed on the sulfurized surface has the shortest H—S bond length (1.362 Å), it is almost not be activated compared to that in the gas phase (1.352 Å), which is also in good agreement with the largest activation free energy (62.0 kJ mol^{-1}).

Above results suggest that H_2S dissociation on the stoichiometric and reduced surface leading to S and H species is likely to be the most favorable compared to that on the sulfurized surfaces, namely, a small quantity of molecular adsorption H_2S can be detected on the sulfurized surfaces, and the stoichiometric surface can be poisoned by S atom. Therefore, H_2S dissociation over CuO(111) surface is a structure-sensitive reaction, the effect of surface structure on the adsorption and dissociation may play an important role in designing high-efficiency H_2S gas sensors.

Finally, as listed in Table 1, Mulliken charge of molecular adsorption H_2S on different CuO(111) surfaces indicate that H_2S emits electrons to surfaces when it interact with surface Cu atoms, our

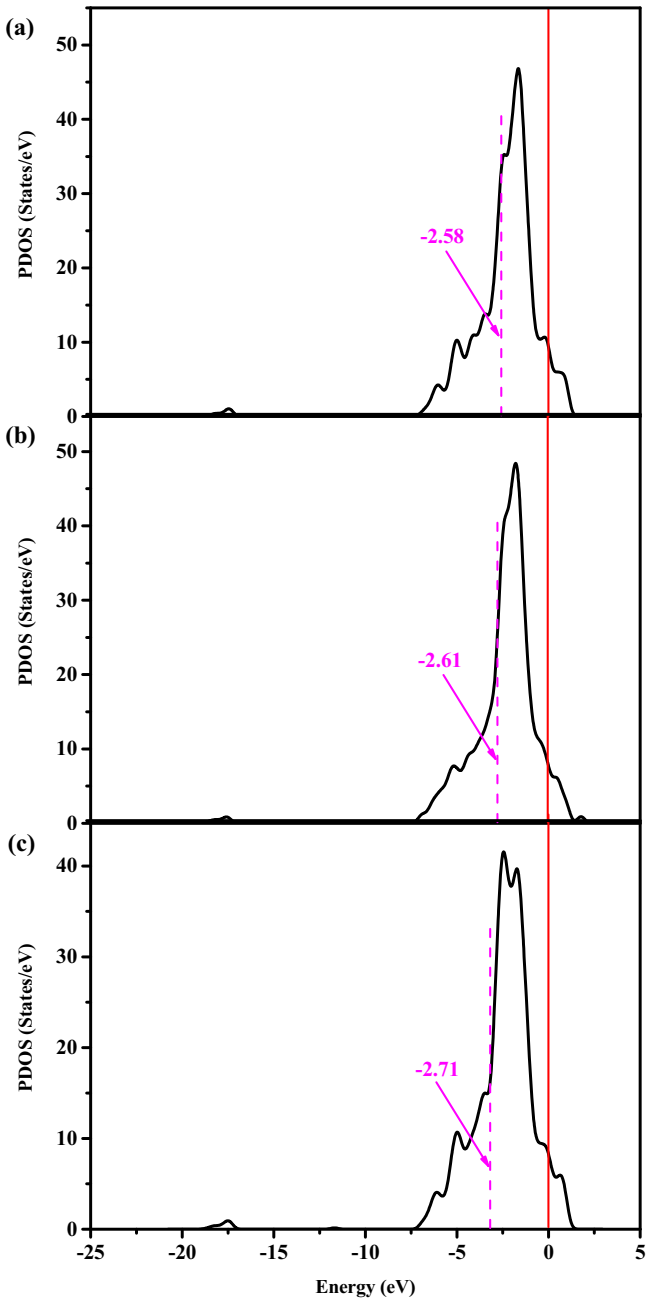

Fig. 7. Projected density of states (pDOS) plots of the *d*-orbitals of the surface Cu atom for three CuO(111) surfaces: (a) Stoichiometric surface, (b) Reduced surface and (c) Sulfurized surface. The vertical dashed lines represent the location of the corresponding *d*-band center. The vertical solid lines indicate the Fermi level.

results agree well with the recent experimental studies [29]. Moreover, all the obtained data of calculated vibrational frequencies of the adsorbed H_2S and SH play an important role in the experimental study, which can provide a systematical theoretical guidance for the adsorption and dissociation of H_2S on other metal oxide surfaces, and illustrate the underlying mechanism for the problem of sulfur poisoning, as well as expand the application of CuO as the high-efficiency H_2S gas sensors.

4. Conclusions

By means of the density functional theory calculations, the mechanism and kinetics of H_2S adsorption and dissociation on different CuO(111) surfaces, including the stoichiometric, reduced

and sulfurized surfaces, have been systematically investigated to probe into the structure sensitivity and the dominant products on CuO(111) surfaces. Our results indicate that H_2S, SH and S species mainly interact with surface Cu atoms via S atom; H_2S can exist in the form of molecular and dissociative adsorption on the stoichiometric, reduced and sulfurized surfaces, and the dissociative adsorption is the main existence form for the first dehydrogenation step of H_2S, which spontaneously dissociate into SH and H species. Meanwhile, since S atom occupies the active center of Cu_{SUB}–Cu_{SUB} bridge site contributing to the dissociative adsorption of H_2S on the stoichiometric surface, the Cu_{SUB}–Cu_{SUB} bridge site cannot lead to the spontaneously dissociation of H_2S on the sulfurized surface, suggesting that the sulfurized surface exhibits a weak catalytic activity toward the dissociation of H_2S compared to that on the stoichiometric surface.

For the complete dissociation of the molecular adsorption H_2S leading to final product S species on these three CuO(111) surfaces, the overall dissociation processes are exothermic, suggesting that the dissociation of H_2S to S and H species is thermodynamically favorable on CuO(111) surfaces; however, the activation free energy of H_2S dissociation on the stoichiometric surface is much smaller than that on the other two surfaces, indicating that the stoichiometric surface exhibits a strong catalytic activity toward H_2S dissociation into S and H species. The sulfur atom acts as a poison on CuO(111) surface, which results in the lower activity toward the dissociation of H_2S. Finally, the vibrational frequencies data for the adsorbed H_2S and SH species on different CuO(111) surfaces provide a systematical theoretical guidance for experimental studies about the surface vibrational spectroscopy.

Acknowledgements

The authors would like to acknowledge the financial support received from the National Natural Science Foundation of China (Grant number 21476155 and 21276171), and the Program for the Top Young Academic Leaders of Higher Learning Institutions of Shanxi, and the Top Young Innovative Talents of Shanxi.

Appendix A. Supplementary data

Supplementary data associated with this article can be found, in the online version, at http://dx.doi.org/10.1016/j.mcat.2017.05.020.

References

[1] G.P. Vissokov, Plasma-chemical preparation of nanostructured catalysts for low-temperature steam conversion of carbon monoxide: properties of catalysts, Catal. Today 89 (2004) 213–221.
[2] G.P. Vissokov, Plasma-chemical preparation of nanostructured catalysts for low-temperature steam conversion of carbon monoxide: catalytic activity, Catal. Today 89 (2004) 223–231.
[3] T. Schedel-Niedrig, M. Hävecker, A. Knop-Gericke, R. Schlögl, Partial methanol oxidation over copper: active sites observed by means of in situ X-ray absorption spectroscopy, Phys. Chem. Chem. Phys. 2 (2000) 3473–3481.
[4] T. Schedel-Niedrig, T. Neisius, I. Böttger, E. Kitzelmann, G. Weinberg, D. Demuth, R. Schlögl, Copper (sub) oxide formation: a surface sensitive characterization of model catalysts, Phys. Chem. Chem. Phys. 2 (2000) 2407–2417.
[5] H.J. Luo, J.Q. Cai, X.M. Tao, M.Q. Tan, Adsorption and dissociation of H_2S on Mo(100) surface by first-principles study, Appl. Surf. Sci. 292 (2014) 328–335.
[6] L.X. Ling, P.D. Han, B.J. Wang, R.G. Zhang, Theoretical prediction of simultaneous removal efficiency of ZnO for H_2S and Hg^0 in coal gas, Chem. Eng. J. 231 (2013) 388–396.
[7] J.G. Speight, Chemistry and Technology of Petroleum, Dekker, New York, 1991.
[8] J. Oudar, H. Wise, Deactivation and Poisoning of Catalysts, Dekker, New York, 1991.
[9] E. Ozdogan, J. Wilcox, Investigation of H_2 and H_2S adsorption on niobium- and copper-doped palladium surfaces, J. Phys. Chem. B 114 (2010) 12851–12858.
[10] D.R. Alfonso, First-principles studies of H_2S adsorption and dissociation on metal surfaces, Surf. Sci. 602 (2008) 2758–2768.
[11] N.S. Ramgir, S.K. Ganapathi, M. Kaur, N. Datta, K.P. Muthe, D.K. Aswal, S.K. Gupta, J.V. Yakhmi, Sub-ppm H_2S sensing at room temperature using CuO thin films, Sens. Actuators B: Chem. 151 (2010) 90–96.
[12] S. Steinhauer, E. Brunet, T. Maier, G.C. Mutinati, A. Kock, O. Freudenberg, C. Gspan, W. Grogger, A. Neuhold, R. Resel, Gas sensing properties of novel CuO nanowire devices, Sens. Actuators B: Chem. 187 (2013) 50–57.
[13] S. Park, S. Park, J. Jung, T. Hong, S. Lee, H.W. Kim, C. Lee, H_2S gas sensing properties of CuO-functionalized WO_3 nanowires, Ceram. Int. 40 (2014) 11051–11056.
[14] E. Laperdrix, G. Costentin, O. Saur, J.C. Lavalley, C. Ńedez, S. Savin-Poncet, J. Nougayŕ edez, Selective oxidation of H_2S over CuO/Al_2O_3: identification and role of the sulfurated species formed on the catalyst during the reaction, J. Catal. 189 (2000) 63–69.
[15] S.J. Sun, D.S. Zhang, C.Y. Li, Y.J. Wang, DFT study on the adsorption and dissociation of H_2S on CuO(111) surface, RSC Adv. 5 (2015) 21806–21811.
[16] A. Galtayries, J.P. Bonnelle, XPS and ISS studies on the interaction of H_2S with polycrystalline Cu: cu_2O and CuO surfaces, Surf. Interface Anal. 23 (1995) 171–179.
[17] J.Y. Lin, J.A. May, S.V. Didziulis, E.I. Solomon, Variable-energy photoelectron spectroscopic studies of H_2S chemisorption on Cu_2O and ZnO single-crystal surfaces: HS-bonding to copper (I) and zinc (II) sites related to catalytic poisoning, J. Am. Chem. Soc. 114 (1992) 4718–4727.
[18] R.G. Zhang, H.Y. Liu, J.R. Li, L.X. Ling, B.J. Wang, A mechanistic study of H_2S adsorption and dissociation on $Cu_2O(111)$ surfaces: thermochemistry reaction barrier, Appl. Surf. Sci. 258 (2012) 9932–9943.
[19] J.A. Rodriguez, A. Maiti, Adsorption and decomposition of H_2S on MgO(100) NiMgO(100), and ZnO(0001) surfaces: a first-principles density functional study, J. Phys. Chem. B 104 (2000) 3630–3638.
[20] T.V. Reshetenko, S.R. Khairulin, Z.R. Ismagilov, V.V. Kuznetsov, Study of the reaction of high-temperature H_2S decomposition on metal oxides (γ-Al_2O_3, α-Fe_2O_3, V_2O_5), Int. J. Hydrogen Energy 27 (2002) 387–394.
[21] L.X. Ling, J.B. Wu, J.J. Song, P.D. Han, B.J. Wang, The adsorption and dissociation of H_2S on the oxygen-deficient ZnO(10-10) surface: a density functional theory study, Comput. Theor. Chem. 1000 (2012) 26–32.
[22] A.D. Mayernick, R. Li, K.M. Dooley, M.J. Janik, Energetics and mechanism for H_2S adsorption by ceria-lanthanide mixed oxides: implications for the desulfurization of biomass gasifier effluents, J. Phys. Chem. C 115 (2011) 24178–24188.
[23] Y.L. Yang, W.K. Chen, C.H. Lu, X. Guo, Density functional theory study of H_2S adsorption and decomposition on cubic $ZrO_2(110)$ surface, Chin. J. Inorg. Chem. 25 (2009) 1457–1463.
[24] S.X. Yin, X.Y. Ma, D.E. Ellis, Initial stages of H_2O adsorption and hydroxylation of Fe-terminated α-$Fe_2O_3(0001)$ surface, Surf. Sci. 601 (2007) 2426–2437.
[25] J. Zhang, R.G. Zhang, B.J. Wang, L.X. Ling, Insight into the adsorption and dissociation of water over different CuO(111) surfaces: the effect of surface structures, Appl. Surf. Sci. 364 (2016) 758–768.
[26] Z. Jiang, M.M. Li, P. Qin, T. Fang, Insight into the adsorption and decomposition mechanism of H_2S on clean and S-covered Au(100) surface: a theoretical study, Appl. Surf. Sci. 311 (2014) 40–46.
[27] S.J. Sun, C.Y. Li, D.S. Zhang, Y.J. Wang, Density functional theory study of the adsorption and dissociation of O_2 on CuO(111) surface, Appl. Surf. Sci. 333 (2015) 229–234.
[28] S.J. Sun, Y.J. Wang, Q.S. Yang, Density functional theory study of the methanol adsorption and dissociation on CuO(111) surface, Appl. Surf. Sci. 313 (2014) 777–783.
[29] J. Dhakshinamoorthy, B. Pullithadathil, New Insights towards electron transport mechanism of highly efficient p-type CuO(111) nanocuboids-based H_2S gas sensor, J. Phys. Chem. C 120 (2016) 4087–4096.
[30] F.A. Filippetti, V. Fiorentini, Magnetic ordering in CuO from first principles: a cuprate antiferromagnet with fully three-dimensional exchange interactions, Phys. Rev. Lett. 95 (2005) 086405-1-4.
[31] F. Ortmann, F. Bechstedt, W.G. Schmidt, Semiempirical van der Waals correction to the density functional description of solids and molecular structures, Phys. Rev. B 73 (205101) (2006) 1–10.
[32] J.P. Perdew, K. Burke, M. Ernzerhof, Generalized gradient approximation made simple, Phys. Rev. Lett. 77 (1996) 3865–3868.
[33] P. Hu, D.A. King, S. Crampin, M.H. Lee, M.C. Payne, Gradient corrections in density functional theory calculations for surfaces: co on Pd(110), Chem. Phys. Lett. 230 (1994) 501–506.
[34] J.P. Perdew, Y. Wang, Accurate and simple analytic representation of the electron-gas correlation energy, Phys. Rev. B: Condens. Matter 45 (1992) 13244–13249.
[35] P. Hohenberg, W. Kohn, Inhomogeneous electron gas, Phys. Rev. 136 (1964) B864–B871.
[36] Y. Inada, H. Orita, Efficiency of numerical basis sets for predicting the binding energies of hydrogen bonded complexes: evidence of small basis set superposition error compared to Gaussian basis sets, J. Comp. Chem. 29 (2008) 225–232.
[37] B. Delley, An all-electron numerical method for solving the local density functional for polyatomic molecules, J. Chem. Phys. 92 (1990) 508–517.
[38] B. Delley, From molecules to solids with the $DMol^3$ approach, J. Chem. Phys. 113 (2000) 7756–7764.
[39] D.E. Jiang, E.A. Carter, Adsorption diffusion, and dissociation of H_2S on Fe(100) from first principles, J. Phys. Chem. B 108 (2004) 19140–19145.
[40] D.R. Alfonso, A.V. Cugini, D.C. Sorescu, Adsorption and decomposition of H_2S on Pd(111) surface: a first-principles study, Catal. Today 99 (2005) 315–322.

[41] E.J. Albenze, A. Shamsi, Density functional theory study of hydrogen sulfide dissociation on Bi-metallic Ni-Mo catalysts, Surf. Sci. 600 (2006) 3202–3216.
[42] D.E. Jiang, E.A. Carter, First principles study of H_2S adsorption and dissociation on Fe(110), Surf. Sci. 583 (2005) 60–68.
[43] E.L. Hardegree, P. Ho, J.M. White, Sulfur adsorption on Ni(100) and its effect on CO chemisorption: I. TDS: AES and work function results, Surf. Sci. 165 (1986) 488–506.
[44] D. Curulla-Ferré, A. Govender, T.C. Bromfield, J.W. Niemantsverdriet, A DFT study of the adsorption and dissociation of CO on sulfur-precovered Fe(100), J. Phys. Chem. B 110 (2006) 13897–13904.
[45] S.D. Miller, J.R. Kitchin, Relating the coverage dependence of oxygen adsorption on Au and Pt fcc(111) surfaces through adsorbate-induced surface electronic structure effects, Surf. Sci. 603 (2009) 794–801.
[46] J.D. Li, E. Croiset, L. Ricardez-Sandoval, Methane dissociation on Ni(100) Ni(111), and Ni(553): A comparative density functional theory study, J. Mol. Catal. A: Chem. 365 (2012) 103–114.